Realistic Performance of LTE

in a macro-cell environment

Jean-Baptiste Landre, Ziad El Rawas, Raphaël Visoz, and Sarah Bouguermouh
Orange Labs
Issy-Les-Moulineaux, France

Abstract—**The aim of this paper is to provide a reliable performance evaluation of 3GPP Long Term Evolution (LTE) networks. A new kind of simulation method, based on drive test measurements on a live network, is used. The measurements are combined with link level simulation results for different LTE device categories. Simulation results show that all MIMO 2x2 LTE devices have the same performance in a macro-cell environment: the average user throughput is around 35Mbps, but there are still differences depending on the user's location. Network upgrade to MIMO 4x4 leads to a 60% improvement of average throughput.**

Keywords: radio access networks, HSPA, LTE, MIMO, CQI.

I. INTRODUCTION AND BACKGROUND

LTE turns out to be a major evolution of wireless networks. LTE technology is expected to come with a significant performance improvement compared to 3G systems, including peak rates of 300Mbps in downlink and 75 Mbps in uplink in 3GPP Release 8, and significant gains in spectrum efficiency. In order to achieve these performances, important changes are made in the radio interface, which is now based on Orthogonal Frequency Division Multiple Access (OFDMA) in the downlink, and Single Carrier Frequency Division Multiple Access (SC-FDMA) in the uplink [1] [2]. OFDM relies on wide bandwidths, up to 20MHz where subcarrier spacing is 15kHz. Modulations up to 64 QAM and channel coding are dynamically selected based on channel quality indicators reported by the devices. Multiple Input Multiple Output (MIMO) is supported from day one by the network. Time-frequency scheduling is performed, with a resource allocation of 1ms x 180kHz.

Although LTE is usually associated to high peak rates, this is for sure not the only figures operators are interested in. First, such throughputs can only be achieved under optimal network conditions: very close to the base station, during off-hours, and in good fading conditions. Second, very few applications can deliver the very high rates of LTE. It is therefore more important that new technology brings an enhancement of the average experienced throughputs, and that includes a relatively uniform distribution of achievable rates across the networks. Those figures do not depend only on the technology: they also depend on network deployment and traffic conditions: sites density, propagation environment, interference conditions, traffic demand distribution, and network optimization have a huge impact on a wireless network performance. All this makes the assessment of the experienced throughput a difficult task. Several previous works evaluated the LTE performance: Studies have been made at the link level, and extended to the system level in [3] [4] [5] [6] [7]. They are based on simplified networks topologies (hexagonal sites grids, typical antenna azimuths and tilts, simplified antenna patterns), and assume uniform traffic load distribution. Such models are good first estimates; however network operators know that things can be very different in live networks. On the one hand, live networks are well planned and have been tuned for a long time. On the other hand, interference conditions are tricky and there can be poor coverage areas because of site acquisition issues, especially in urban areas. In parallel with the simulations, field trials and then drive tests on the first live networks have been reported in [8] and [9]. However, field trials are performed with a limited number of radio sites, and a few terminals resulting in non realistic low interference conditions. Regarding LTE live networks, they are still in a deployment phase: the network loads is very low, and neither the radio sites acquisition process nor the RF optimization work have been completed. Furthermore, both field trials and drive tests on live networks provide results that are of course limited to networks and devices that are commercial equipments, or prototypes made available by the industry: performance of mid and long-term evolutions planned by the standards cannot be assessed this way.

This paper proposes a method to estimate LTE performances of present and future devices, based on radio inputs from 3G live networks (loaded, with actual traffic distribution, optimized, and for which the site acquisition process is close to completion) combined with link-level simulations. The document is organized as follows. In section II, the link level receiver structures are presented in section III. Simulation scenarios and results are presented and discussed in section IV.

II. LINK LEVEL RECEIVER MODELLING

A. System model

MIMO *2x2* and MIMO *4x4* transmission schemes are evaluated in this paper. The number of transport blocks (TBs) that can be transmitted independently varies between one or two upon the number of available spatial layers which can not exceed $min\,(N_r, N_t)$, where N_r is the number of receive antennas and N_t the number of transmit antennas. Each TB is carried by at least one dedicated spatial layer. The l spatial layers are finally precoded by a $N_t \; x \; l$ matrix **W**. The LTE MIMO channel processing is given in Fig. 1. The choice of the TB format(s), the number of spatial layer(s) and precoding matrix is given by the closed loop feedback which is derived at the terminal side in order to maximize the data rate for a given BLock Error Rate (BLER).

978-1-4673-0990-5/12/$31.00 ©2012 IEEE

A TB format corresponds to a specific MCS (Modulation and Coding Scheme).

In this paper, it is assumed that the eNode B always follows the UE recommendations.

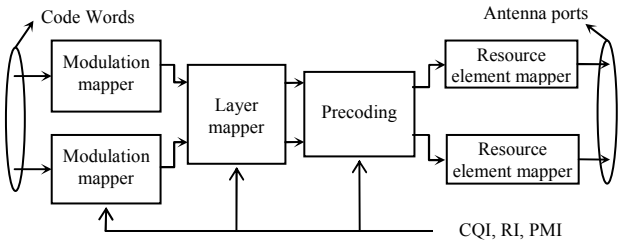

Figure 1. *Overview of physical channel processing*

The OFDM received signal for a given Physical Resource Block (PRB) k can be written as:

$$\boldsymbol{y}_{k,l} = \boldsymbol{H}_k \boldsymbol{W}_l \boldsymbol{x}_k + \boldsymbol{n}_k = \boldsymbol{H}_{0,k,l} \boldsymbol{x}_k + \boldsymbol{n}_k \qquad (1)$$

where $\boldsymbol{x}_k=[x_{k,1} \dots x_{k,l}]^t$, $\boldsymbol{y}_k=[y_{k,1} \dots y_{k,N_r}]^t$, $\boldsymbol{n}_k$ is the AWGN noise vector with covariance $\sigma^2 \boldsymbol{I}_{Nr}$ ($\boldsymbol{I}_{Nr}$ being the identity matrix of dimension N_r) and $\boldsymbol{H}_k$ is the $N_r \, x \, N_t$ flat MIMO channel of the PRB k. The latter is assumed to be constant during one TTI. The precoding matrices that can be applied to the spatial layers are stored in a codebook known by the UE and eNode B. The precoding codebook is presented in [11].

B. LMMSE equalizer

For the sake of notation simplicity, we remove the index k since the linear processing is the same for each PRB. By denoting $\boldsymbol{F}$ the Linear MMSE filter, it yields to

$$\boldsymbol{F}_l^H = \boldsymbol{H}_{0,l}^H \left[\boldsymbol{H}_{0,l} \boldsymbol{H}_{0,l}^H + \left(\frac{\sigma^2}{\varepsilon} \right) \boldsymbol{I} \right]^{-1} \qquad (2)$$

The LMMSE estimate $\boldsymbol{z}_l$ is given by:

$$\boldsymbol{z}_l = \boldsymbol{F}_l^H \boldsymbol{y}_l = \boldsymbol{F}_l^H \boldsymbol{H}_{0,l} \boldsymbol{x} + \boldsymbol{F}_l^H \boldsymbol{n} \qquad (3)$$

The LMMSE SINR [12] [13] associated to spatial layer $n \leq l$ is:

$$\gamma_{l,n} = \left[\left(\frac{snr}{\left(\left(\boldsymbol{H}_{0,l}^H \boldsymbol{H}_{0,l} + \frac{1}{snr} \boldsymbol{I}_l \right)^{-1} \right)_{n,n}} \right) - 1 \right] \qquad (4)$$

The channel and the precoding are assumed to be perfectly known at the receiver.

C. Link adaptation

The link adaptation is performed every TTI. Based on the feedback from the UE (CQI: Channel Quality Indicator, PMI: Precoding Matrix Indicator, RI: Rank Indicator), it consists of adapting the modulation and coding scheme of each TB, choosing the optimal precoding matrix and fixing the rank indicator (or number of supported spatial layer(s)). In this paper, we only consider Chase Combining for retransmission. Moreover, the radio channel is assumed to be constant during one (codeword) transmission and changes independently from one transmission to the other (i.e., quasi –static assumption). By different transmissions, we mean here different payloads. On the other hand, the radio channel is assumed to be the same as the one experienced by the first transmission for the subsequent retransmissions, i.e., the same TB is used for retransmissions. These assumptions are strictly valid when the retransmission round trip time delay does not exceed the coherence time of the channel (which is true for low to medium UE mobility).

The transmission scheme varies between two modes (transmission mode 4 and 6 defined in [1]):

- Closed Loop Precoding Rank 1 and
- Closed Loop Precoding Spatial Multiplexing.

Since only one UE uses the total bandwidth, feedbacks for sub-band CQI are useless. As a result, the reporting mode 1-2 [1], which is based on wideband CQI and sub-band PMI is selected in this paper.

The link adaptation algorithms rely on the Mutual Information Effective SINR Mapping (MIESM) technique as described in [13] [14]. As the codeword will be spotlighted by different subcarrier SINR, this technique allows us to compress these multiple SINRs into a single effective $SINR_{eff}$ *as* follows:

$$SINR_{eff} = I_Q{}^{-1} \left(\frac{1}{P} \sum_{p=1}^{P} I_Q(SINR_p) \right) \qquad (5)$$

Where $I_Q(SNR)$ is the mutual information discrete-entries (modulation Q dependent) for an AWGN channel.

Fast link adaptation can be summarized into two algorithms: The first one consists of selecting the optimal precoding matrix over a sub-band, and the second one uses the previously computed SINR with the selected precoding matrices to select the TB formats and the rank indicator.

1) PMI selection: The optimal precoding matrix corresponds to the one that maximizes the mutual information over the sub-band. Since the precoding matrix selection procedure is modulation independent, we assume the highest modulation to select the optimal precoding matrix as in [13]. The matrix is selected by the UE for each sub-band and number of spatial layers. The subband size depends on the bandwidth. We approximate the size by taking always 5 PRB. The PRB SINRs within a sub-band are used to compute the mutual information which is then compared for all available precoding matrices. The precoding matrices that maximize the sum of the mutual information over all spatial layers and PRBs within a sub-band are selected.

2) CQI and Rank selection: The CQI is evaluated over the whole bandwidth. The UE estimates for each codeword the transmission mode and the modulation to be used depending on the effective SINR. For each possible modulation (QPSK, 16QAM, 64 QAM) and coding rate (defining a TB), there is a corresponding LUT (Look Up Table)that is simulated off-line on a AWGN channel, and that assigns an SNR to each BLER value. Based on the $SINR_{eff}$ computed over the whole bandwidth conditional on the selected precoding matrices in step 1, the best TB format that should ensure a BLER lower than 10% while maximizing the data rate, is selected. In case of two TBs, the overall data rate is the sum of each TB throughput. The selection procedure aims at maximizing the overall data rate.

3) Algorithms for Fast Link Adaptation: Fast Link adaptation relies on two algorithms to select the optimal precoding matrices and the appropriate transport block(s).

a) Algorithm 1: Selecting the precoding matrices

The algorithm inputs are the Channel matrices, the precoding codebook, the Mutual Information LUTs.

1. **for** $l = 0$ ... $\min\{N_r, N_t\} - 1$ **do** */ N_l: maximum number of layers*
2. **for** $b = 0 \ldots N_{sb} - 1$ **do** */ N_{sb}: number of sub-band*
3. **for** $w = 0 \ldots N_{w,l} - 1$ **do** */ $N_{w,l}$: number of pre-coding matrices*
4. **for** $p = 0 \ldots N_{prb} - 1$ **do** */ N_{prb}: Number of PRB within a subband*
5. **for** $n = 0 \ldots l - 1$ **do** */ n : spatial stream indicator*
6. Compute $SINR_{l,w,n}^{k(b,p)=N_{prb}b+p}$
7. **end for**
8. Compute $I_{l,w}^{b,p} = \frac{1}{l}\sum_{n=0}^{l-1} I(SINR_{l,w,n}^{b,p})$
9. **end for**
10. Compute $I_{l,w}^{b} = \frac{1}{N_{prb}}\sum_{p=0}^{N_{prb}-1} I_{l,w}^{b,p}$ */ MI per sub-band b for precoding w*
11. **end for**
12. $\mathrm{w_l^b} = \mathrm{argmax}_w(I_{l,w}^b)$ */ precoding index for suband b and l spatial layers*
13. **end for**
14. **end for**

Outputs: $\left\{SINR_{l,w_l^b,n}^{k}\right\}$ *and* $\left\{\mathrm{w_l^b}\right\}$

b) Algorithm 2: Selecting TB formats and Rank

The SINR Computed by the first algorithm, the AWGN LUT and the Mutual information LUT are the inputs.

1. **for** $l = 0$ ... $\min\{N_r, N_t\} - 1$ **do**
2. **for** Q =0 … M-1 **do** */ M: modulation type*
3. **for** n =0 … $l - 1$ **do**
4. **for** k=0 …. $N_{tot} - 1$ **do** */ N_{tot}: total number of PRB in the system*
5. Compute $I_{Q,l,n}^{k} = I_Q(SINR_{l,w_l^b,n}^{k})$ */ Compute MI for a each stream*
6. **end for**
7. **end for**
8. **If** l =1 */ Layer 1*
9. $N_{CW} = 1$ */ N_{CW}: number of codeword*
10. $SINR_{eff}^{1,1,Q} = {I_Q}^{-1}\left(\frac{1}{N_{tot}}\sum_{k=0}^{N_{tot}-1} I_{Q,1,1}^{k}\right)$
11. **end if**
12. **If** l =2 */ Layer 2*
13. $N_{CW} = 2$
14. $SINR_{eff}^{1,2,Q} = {I_Q}^{-1}\left(\frac{1}{N_{tot}}\sum_{k=0}^{N_{tot}-1} I_{Q,2,1}^{k}\right)$
15. $SINR_{eff}^{2,2,Q} = {I_Q}^{-1}\left(\frac{1}{N_{tot}}\sum_{k=0}^{N_{tot}-1} I_{Q,2,2}^{k}\right)$
16. **end if**
17. **If** l =3 */Layer 3*
18. $N_{CW} = 2$
19. $SINR_{eff}^{1,3,Q} = {I_Q}^{-1}\left(\frac{1}{N_{tot}}\sum_{k=0}^{N_{tot}-1} I_{Q,3,1}^{k}\right)$
20. $SINR_{eff}^{2,3,Q} = {I_Q}^{-1}\left(\frac{1}{2\times N_{tot}}\sum_{k=0}^{N_{tot}-1}(I_{Q,3,2}^{k} + I_{Q,3,3}^{k})\right)$
21. **end if**
22. **If** l =4 */Layer 4*
23. $N_{CW} = 2$
24. $SINR_{eff}^{1,4,Q} = {I_Q}^{-1}\left(\frac{1}{2\times N_{tot}}\sum_{k=0}^{N_{tot}-1}(I_{Q,4,1}^{k} + I_{Q,4,2}^{k})\right)$
25. $SINR_{eff}^{2,4,Q} = {I_Q}^{-1}\left(\frac{1}{2\times N_{tot}}\sum_{k=0}^{N_{tot}-1}(I_{Q,4,3}^{k} + I_{Q,4,4}^{k})\right)$
26. **end if**
27. **for** c=1 **…** N_{CW} */ c: codeword indicator*
28. Select best $TB^{c,l,Q}$ from $LUT_{TB,BLER}(SINR_{eff}^{c,l,Q})$
29. **end for**
30. **end for**
31. **for** c=1 **…** N_{CW}
32. $Q_0 = \underset{Q}{\mathrm{argmax}}\ \mathrm{Throughput}(TB^{c,l,Q})$
33. $D_{c,l} = \mathrm{Throughput}\ (TB^{c,l,Q_0})$
34. **end for**
35. Compute $D_l = \sum_{c=1}^{N_{CW}} D_{c,l}$
36. **end for**
37. $\mathrm{l_0} = \underset{l}{\mathrm{argmax}}\ \mathrm{D_l}$

Outputs: $\{TB^{c,l_0,Q_0}\}, D_l$ *and* $Rank = l_0$

D. Radio Channel

Pedestrian-A channel defined in [15] is the radio channel applied. We consider that the transmit antenna are correlated with a coefficient α=0.5 and the correlation at the receiver coefficient is β=0.2. The correlated MIMO channel tap's H can be expressed as [10]:

$$H_l = R_{Nr}^{1/2} H_l R_{Nt}^{1/2} \qquad (6)$$

III. EVALUATING PRESENT AND FUTURE LTE DEVICES

A. Outline

We showed in [16] and [17] a method for HSDPA performance simulations that combines simulations at link level with drive test measurements carried out with scanner equipment on the 3G live network. [18] has confirmed the need to use measurement on existing deployment to assess the LTE performance. This paper provides a method to obtain an estimate of LTE performance based on measurements on the live HSPA network, combined with LTE link-level simulations. The key advantage of this method is that it provides a picture of LTE networks as they will be in the future: densified, optimized, and loaded. LTE radio equipments are indeed progressively co-sited with the existing 3G equipments, sharing masts and having similar antenna settings: in the long run, each radio site of today's network will have LTE equipments. Furthermore, another advantage of this method is that all LTE devices categories, existing ones but also future ones, can be simulated with the same radio inputs, which allow apple to apple comparison between them. Reliable performance predictions of future technology can then be achieved before deploying it. This can be a key input for strategic decision making. For example 4x4 MIMO has a high impact on the radio access network: it requires expensive hardware upgrade on a large scale, including antennas swaps, and transmitter chains additions. Therefore, insights into the benefits from new technology before rolling it out are key elements.

B. Available measurements

All 3G drive tests made with a scanner provide CPICH received signal code power (RSCP) and E_c CPICH/I0, which is the received chip energy relative to the total power spectral density I_0. The advantage of the scanner is that a huge amount of samples can be collected, thereby providing performance information for whole cities.

C. RSRP calculation

RSRP is comparable to the CPICH RSCP measurement in WCDMA. RSRP is the linear average (in watts) of the downlink reference signals (RS) across the channel bandwidth [19]. An accurate estimate of the RSRP value can be calculated from the measured RSCP with

$$RSRP_{5MHz} = RSCP + 10log\left(\frac{RS\ Tx\ power}{CPICH\ Tx\ power}\right) + \Delta_{pl} + \Delta_{lb} \quad (7)$$

Where Δ_{pl} is the over-the-air path loss difference between the different carrier frequencies that are used for systems, and Δ_{lb} is the link budget difference between LTE and HSPA. Δ_{lb} includes Node B and device antenna gains, receiver's noise figure, and feeder loss differences. Antenna patterns of the

radio sites and devices might indeed be different, and could be considered in the calculations above. However, the usual cell planning strategy for the antennas of new wireless systems consists in reusing existing sites and deploying antennas that have similar size and beam widths, with the same antenna azimuths and tilt settings. So we can make the assumption that transmit and receive antenna gains are the same for both technologies.

D. LTE inter-cell interference calculations

As we want a picture of a mature and loaded LTE network, we make two other assumptions: first we consider that the LTE site acquisition process has been completed, and that one LTE NodeB is co-sited with one 3G NodeB; second we assume that the traffic demand is similar to the current 3G one, in terms of volume but also in terms of traffic geographical distribution. A good estimate of the other-cell interference for LTE I_{oc} on 5 MHz is then:

$$I_{oc_{5Mhz}}^{LTE} = I_{oc}^{HSPA} + 10log\left(\frac{Tx\ power_{5MHz}^{LTE}}{Tx\ power^{HSPA}}\right) + \Delta_{pl} \quad (8)$$

Where $Tx\ power_{5MHz}^{LTE}$ is the average transmit power of the LTE NodeBs on a 5 MHz bandwidth and $Tx\ power^{HSPA}$, the average transmit power of the 3G NodeBs on the live network.

The interference signal power is then calculated simply writing: $$I_o = I_{oc} + N_o \quad (9)$$

Where I_{oc} is the inter-cell interference on 20 MHz, calculated from $I_{oc_{5Mhz}}^{LTE}$, and N_o the noise power, which depends on the receiver noise figure.

E. Downlink SCH received power and signal to noise ratio

The received power for the downlink shared channel (DL-SCH) is calculated from the pilot received signal, and from the transmit power offset between the DL-SCH channel and the CPICH. Since all the channels go through the same propagation channel, the power offsets at the receiver's side are the same as the power offsets defined at the transmitter's side, which are known.

$$Rx\ power^{DSCH} = RSRP + 10\ log\left(\frac{Max\ Tx\ power^{DSCH}}{Tx\ power^{RS}}\right) \quad (10)$$

Again, the calculation is possible because the power offsets between reference signals and DL-SCH are the same at the receiver's side and at the transmitter's side, the latest being known. DL-SCH signal to noise ratio is then calculated with

$$SNR^{DSCH} = \frac{Rx\ power^{DSCH}}{I_o} \quad (11)$$

F. Throughput calculation

Throughput is then directly obtained from SNR^{DL-SCH} using lookup tables from the link-level simulations. The correspondence is done by identifying each computed SNR (11) to the link level one, and the optimal throughput, provided by the link level look-up tables, is hence selected.

IV. Simulation scenarios and result

A. Scenarios and Drive test measurements

The main LTE release 8 categories have been simulated: categories 2 (50Mbps-capable), 3 (100Mbps), 4 (150Mbps), and 5 (300Mbps). Category 2, 3 and 4 support MIMO 2x2 ones, and category 5 supports MIMO 4x4 ones. A measurement campaign of the 3G metrics has been run recently in the centre of a major European town. The drive test area is around 105 sq. kms. Most of the sites that have been rolled out in that area have three sectors, but some of them have two sectors, and a few ones have four sectors. Measurements are available for hundreds of cells. Inter-site distance is low because 3G sites have been built on a densified GSM network. Interference conditions are tricky because of irregular propagation and because of multi-paths. 250 000 drive test samples have been collected. They have been made with scanner equipment embedded in a drive test vehicle. This scanner is connected to an antenna located on the roof of the vehicle. The results are combined to link level outputs respecting the parameters described in table I. Power budgets for HSPA and LTE transmitters are given in Table 1.

TABLE I. Downlink power budget parameters

Parameter	HSPA	LTE
Carrier bandwidth	5 MHz	20 MHz
Base station maximum transmit power	33W	2x30W
Pilot/reference signal power	1.3W	2x3W
Other control channels power	1.3W	2x3W

Downlink link budget parameters are given in Table 2 for both LTE and HSPA. Extensive carrier wave (CW) measurements in live networks in urban areas for different frequency bands [20] have come to the conclusion that the average path loss difference between 2.1 GHz and 2.6GHz is 3 dB. We assume that Remote Radio Heads are deployed for all LTE sites, which suppress the feeder loss.

TABLE II. Downlink link budget parameters

Parameter	HSPA	LTE
Feeder loss	2dB	0dB
Carrier frequency	2.1 GHz	2.6 GHz
Mobile noise figure	7 dB	7 dB
Mobile antenna gain	0 dBi	0 dBi
Body loss	4dB	4dB
Penetration margin (indoor window)	9dB	10dB
Noise figure	7dB	7dB
Over-the-air propagation offset	0dB	3dB

V. Simulation results and discussion

A screenshot of the LTE "virtual" drive test for category 5 devices is shown in Figure 2. This plot shows that there is a high diversity of figures, all along the drive test road: LTE is not a fair technology since users close to the radio site can expect high throughputs in average, while users at the cell edge achieve lower throughputs. The complementary cumulative density functions (CCDF) for the different categories are shown in Figure 3. It turns out that all MIMO 2x2 categories (2, 3 and 4) have the same performances. The reason is that the higher LTE categories require high signal to noise figures to

provide significant performance improvement on the user experienced throughputs, which are not achieved on the network. On the other hand, category 5 devices, that support 4x4 MIMO, outperform the 2x2 categories: the average throughput is 60% better, performances are improved at cell center, and in the other locations of the cell, including the cell edge.

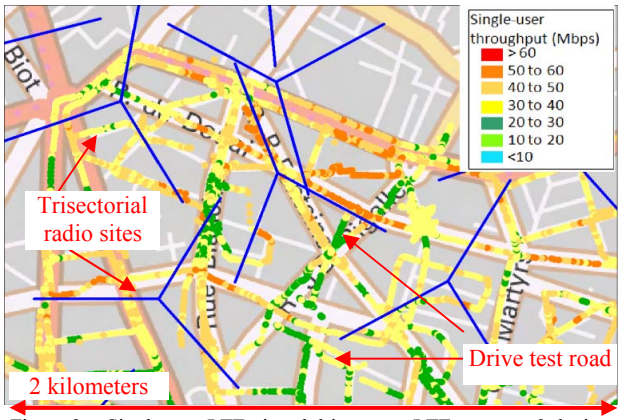

Figure 2. Single user LTE virtual drive test – LTE category 3 device

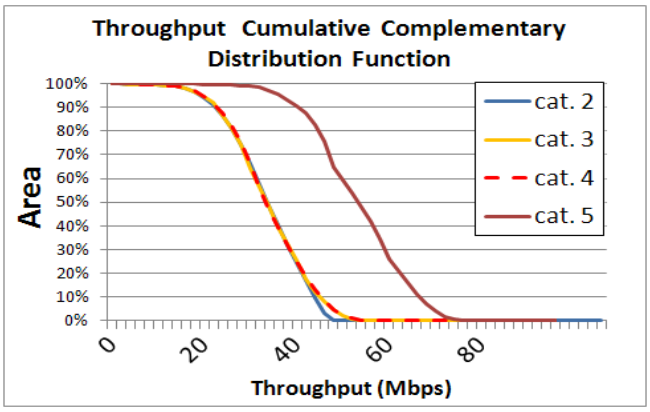

Figure 3. Throughputs statistics for LTE devices categories

Figure 4 shows the average throughput on the drive test, the cell edge throughput (defined as the 5th percentile of the throughput statistics), and the cell center throughput (defined as the 95th percentile of the statistics).

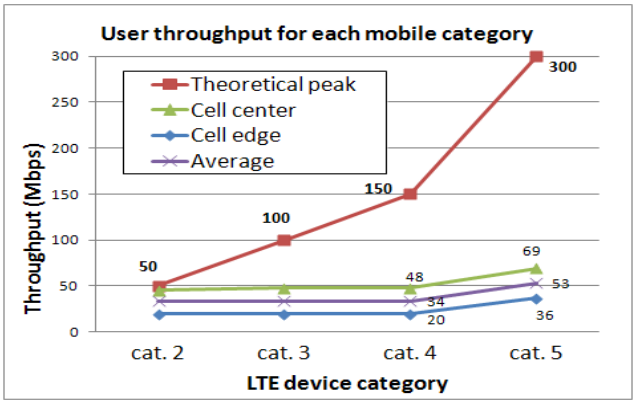

Figure 4. Throughputs comparison between LTE devices categories

For all categories, the throughputs are below the devices peak throughputs, even at cell center. Although there is still a big difference between the cell edge and at the cell center figures, the user throughputs achieved at the cell edge are good.

VI. CONCLUSION

Realistic performance of LTE release 8 devices are shown in this paper. Experienced throughputs in mature LTE networks turn out to be significantly higher than what is experienced with 3G technology. However, they remain lower than the advertised peak throughputs, and depend on the user's location in the network, although good throughputs are achieved at cell edge. All LTE MIMO 2x2 categories have similar performances in the macro-cell network, but MIMO 4x4 provides a significant gain for all locations in the network.

REFERENCES

[1] 3GPP Technical Specification 36.213 "Physical layer procedures (FDD)", v8.8, 29/09/2009

[2] E. Dahlman, A. Furuskär, Y. Jading, M. Lindström and S. Parkvall, "Key features of the LTE radio interface", Ericsson Review n°2, 2008

[3] H. Holma, A. Toskala, "WCDMA for UMTS: HSPA Evolution and LTE", 4th edition, 2007.

[4] H. Holma, A. Toskala, "LTE for UMTS, OFDMA and SC-FDMA based radio access", 2009

[5] A. Furuskär, T. Jönsson, M. Lundevall, "The LTE radio interface, key characteristics and performances", Proc. IEEE PIMRC 2008

[6] S. Kumar et al. ,"Performance evaluation of 6-sectors-site deployment for downlink UTRAN Long term evolution", Proc. VTC Fall 2008

[7] F. Athley, M. Johansson, "Impact of electrical and mechanical antenna tilt on LTE downlink system performance", Proc. VTC Spring 2010

[8] K. Werner, J. Furuskog, M. Riback, B. Hagerman, B, "Antenna configurations for 4x4 MIMO in LTE - Field Measurements", Proc.VTC Spring 2010

[9] M. Thelander, " LTE eNodeB Scheduler Performance", Signals ahead review n°11, 2010

[10] R. Visoz, & all, "Frequency-domain block turbo-equalization for single-carrier transmission over mimo broadband wireless channel", IEEE ICC, VOL. 54, N°. 12, dec 2006.

[11] 3GPP Technical Specification 36.211 V8.9.0 - Physical Channels and Modulation, 12/2009.

[12] E. Zimmermann & G.Fettweis, "Adaptive vs. hybrid iterative mimo receivers based on mmse linear and soft-sic detection", IEEE 17th International Symposium, 2006.

[13] E. Ohlmer & G. Fettweis, "Link adaptation in linearly precoded Closed-Loop MIMO-OFDM systems with linear receivers", IEEE ICC, 2009.

[14] A.M. Cipriano, R. Visoz and T. Sälzer, "Calibration issues of phy layer abstractions for wireless broadband systems", IEEE, VTC Fall 2008.

[15] 3GPP Technical Specification 36.101 V8.12.0 - User Equipment (UE) radio transmission and reception-Annex B, 12/2010.

[16] A. Saadani, J.B. Landre, "Realistic Performance of HSDPA Evolution 64-QAM in Macro-Cell Environment", Proc. IEEE VTC spring 2009

[17] J.B. Landre, A. Saadani, F. Ortolan, "HSDPA radio capacity improvement with advanced devices", IEEE VTC-spring 2010

[18] A. Simonsson et al., "LTE downlink inter-cell interference assessment in an existng GSM metropolitan deployment", Proc. VTC Fall 2010

[19] 3GPP Technical Specification 36.214 v8.0.0 "Physical layer measurements", 09/2007

[20] L. Chaigneaud, JC Kling, "Reference propagation offsets in different frequency bands" Orange Labs internal report, 2011